Proceedings of the 11th World Congress on Mechanical, Chemical, and Material Engineering (MCM'25)

Paris, France - August, 2025 Paper No. HTFF 196 DOI: 10.11159/htff25.196

Topology-Optimized Indirect Cooling System for Thermal Management of Cylindrical Li-Ion Battery Packs

Nicola Bianco¹, Rosa Francesca De Masi², Andrea Fragnito¹, Marcello Iasiello¹, Gerardo Maria Mauro³, Vittorio Orlanducci², Francesco Piccirillo¹

¹Università degli Studi di Napoli Federico II, Department of Industrial Engineering Piazzale Tecchio 80, 80125 Napoli, Italy

nicola.bianco@unina.it; andrea.fragnito@unina.it; marcello.iasiello@unina.it; francesco.piccirillo@unina.it

²Università degli Studi del Sannio, Department of Engineering

Piazza Roma 21, 82100 Benevento, Italy

rfdemasi@unisannio.it; vorlanducci@unisannio.it

3Università degli Studi di Napoli Federico II, Department of Architecture
Via Forno Vecchio 36, 80134, Napoli, Italy
gerardomaria.mauro@unina.it

Abstract - This study introduces an innovative thermal management system for cylindrical Li-ion battery packs, designed to control temperature rise during standard operation while maintaining a uniform temperature distribution. The proposed system employs an indirect cooling approach, utilizing channels that circulate water as the heat transfer fluid. These channels are thermally coupled to the batteries via an aluminium cold plate, which serves as both thermal spreader and structural support. Notably, the metal support integrates the cooling channels without direct battery contact, serving as conductive path for heat dissipation. The analysis focuses on a Sony 18650 cylindrical battery, with a nominal capacity of 2.7 Ah and a voltage of 3.6 V. Heat transfer performance is evaluated using Bernardi's thermal model at a C-rate of 10. To address the high weight of the metallic cold plate, a topology optimization (TO) approach is implemented to identify the material distribution that allows the battery to effectively dissipate thermal power into the heat transfer fluid while reducing the system's weight. This redesigned component achieves an 80% weight reduction compared to the baseline metal spreader, with a minimal trade-off of a 1°C increase in temperature rise. The results underscore the potential of topology optimization to generate practical designs that facilitate efficient battery thermal management systems.

Keywords: Li-ion battery; thermal management; topology optimization; indirect cooling

1. Introduction

Renewable energy sources are consolidated sustainable solution for meeting energy needs without harming the environment. However, their large-scale implementation faces significant challenges, primarily due to their intermittent nature. Efficient energy storage systems are crucial to addressing these issues, with batteries playing a pivotal role in managing and storing electrical energy effectively. A key challenge associated with batteries is thermal management. In applications such as electric vehicles (EVs), smartphones, and computers, maintaining optimal operating temperatures is critical to ensure both the safety of users and the longevity of the batteries themselves. For instance, batteries have an optimal temperature range between 15 and 30 °C with a maximum temperature difference among the batteries, that form the battery pack, less than 5 °C [1]. The thermal challenges in batteries can be categorized based on temperature conditions. Low-temperature issues are common in regions with environmental temperatures below 0 °C, such as Russia and Canada, where battery performance is negatively impacted, resulting in reduced discharge rate, capacity, and state of charge. High-temperature issues, on the other hand, can lead to a dangerous phenomenon known as thermal runaway, which occurs when the battery's operating temperature exceeds the critical threshold of 50-60 °C [2]. When the temperature exceeds the established limit, the battery begins to degrade due to uncontrolled exothermic reactions, causing a rapid increase in temperature. This phenomenon, known as thermal runaway, is a major cause of accidents, especially in electric vehicles (EVs), making it essential to implement an efficient thermal management systems.

exist, such as PCM systems with or without fins, direct or indirect fluid systems, and natural or forced convection. This paper will focus on the indirect fluid system. PCM-based systems offer several advantages, including being passive (requiring no energy to circulate the fluid) and utilizing latent heat during phase transitions. However, one of the main drawbacks is low thermal conductivity, which can be partially addressed by adding fins, though this adds weight [3]. Experimental studies on natural and forced convection systems have shown that while these are among the simplest and least expensive, they have lower heat transfer capacity than other systems, limiting their ability to sufficiently reduce and uniform temperature, which makes them less common in battery applications [4]. On the other hand, direct fluid systems are highly effective at reducing battery temperature and creating uniform thermal fields due to direct contact between the fluid and the battery. However, they require significantly more energy to move the large fluid flow rate and are the heaviest systems overall. Additionally, insulating materials or non-conductive fluids, such as dielectric oils, are needed to prevent electrical short circuits [5]. Some studies have introduced improved direct systems with specific insulating configurations, while others have explored different dielectric fluids to enhance efficiency [6]. This paper will focus on indirect fluid systems, which do not require insulating materials, avoid direct contact, and use less energy and weight compared to direct fluid systems. These systems can dissipate more heat than air systems but less than direct systems due to indirect contact between the fluid and the batteries. One such system uses cold plates made of aluminum, with fluid flowing through channels inside these plates. While the fluid does not make direct contact with the batteries, which reduces heat transfer efficiency, the system can be optimized for better performance [7]. To enhance this system's efficiency, topology optimization has been applied to redesign the channel configuration inside the cold plates. Hybrid systems that combine various methodologies, such as channels and forced convection, have also been developed to improve thermal efficiency while reducing costs and weight [8]. These systems, though more effective at reducing battery temperature and creating a uniform thermal field, are heavier and more expensive, limiting their suitability for applications like EVs [9]. For this reason, topology optimization (TO) can be implemented to reduce the use of material and consequently the weight and cost searching to maintain thermal efficiency. Therefore, topology optimization has been employed to minimize material use, thereby reducing both weight and cost while maintaining thermal efficiency [10]. This work applies TO to an indirect battery pack cooling system, with the aim of reducing the amount of solid material while preserving the thermal management performance.

2. Materials and methods

This section provides an overview of the thermal management system, beginning with the core component of the device – the cylindrical battery – by outlining its geometry and thermal model. Subsequently, we describe the configuration of a battery pack, which will serve as the baseline solution in the following analysis.

2.1 Thermal management problem

The analysis of the battery pack begins from its main component: the cylindrical battery. The battery analysed is a SONY 18650 model, having a height (H) of 65 mm and a diameter (D) of 18 mm. The battery consists of four components: core, positive pole, negative pole and positive plate, whose thermophysical properties – taken from the literature [11] – are listed in Tab. 1. In particular, the core thermal conductivity k has an anisotropic behaviour, equal to 1.6 W/(mK) in the radial direction, and 3 W/(mK) in the axial direction, respectively. A schematical overview of the cylindrical battery is provided in Fig. 1.

Table 1: Thermophysical properties of the battery components

Component	c (J/kgK)	k (W/mK)	ρ (kg/m ³)	$R (m\Omega)$	$V(\text{mm}^3)$	H(mm)	D (mm)
Core	900	3 / 1.6	2000	18	1650	65	18
Positive pole	903	238	2710	$2.20 \cdot 10^{-3}$	12.7	2.0	9.0
Negative pole	460	20.0	7900	$3.96 \cdot 10^{-3}$	3.93	0.5	10
Positive plate	903	238	2710	9.79 ·10-4	5.65	0.5	12

c, ρ , R, V are the specific heat, the density, the electric resistance and the volume of the battery, respectively.

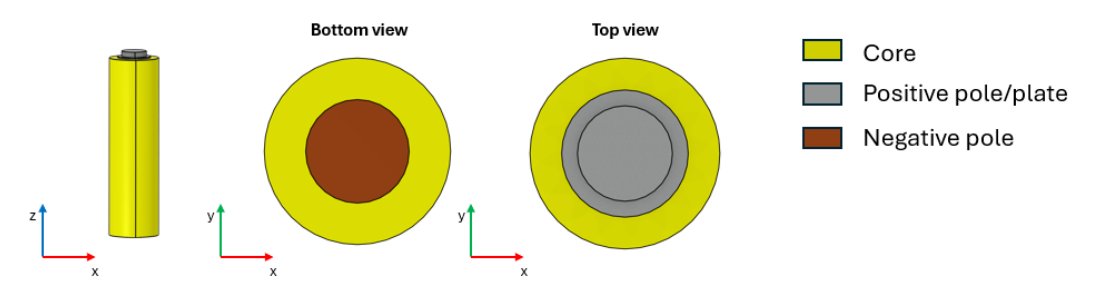


Fig. 1: Cylindrical battery: geometry and views

To calculate the temperature field, the battery heat generation (Q_t) must be evaluated inside it. The core heat generation is dependent from two different rates: the reversible (Q_{rev}) , and the irreversible one (Q_{irr}) . The former is based on Bernardi's model [11] and includes all the exothermic and endothermic heat generations due to chemical reactions occurring within the battery, and it is a function of the entropic coefficient (dU/dT), measured experimentally [12]. The irreversible heat generation is related to Joule heating effects. For the other components, only irreversible heat generation is considered, because no chemical reactions take place inside them.

$$Q_{t} = Q_{rev} + Q_{irr} = \frac{I^{*} T^{*} \frac{dU}{dT}}{V} + \frac{R^{*} l^{2}}{V}$$
 (1)

In Eq. (1) the term I represents the current value and T the temperature. The temperature fields are calculated for the fluid and solid domains, where the convective term $(\rho c_p u \cdot \nabla T)$ is zero inside the solid domains. The velocity field for the fluid domains is evaluated coupling also momentum and continuity equations.

$$\rho c_p \frac{\partial T}{\partial t} + \rho c_p u \cdot \nabla T - \nabla k (\nabla T) = Q_t$$
 (2)

$$\rho \frac{\partial u}{\partial t} + \rho (u \cdot \nabla) u = - \nabla p + \mu \nabla^2 u \tag{3}$$

$$\rho \nabla \cdot u = 0 \tag{4}$$

Where t, μ , p and u are the time, dynamic viscosity, the pressure and the velocity of the fluid respectively.

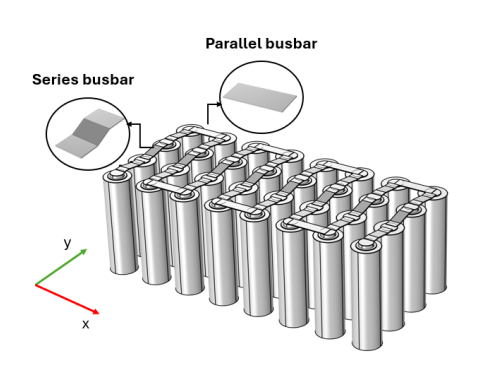
2.2 Baseline solution

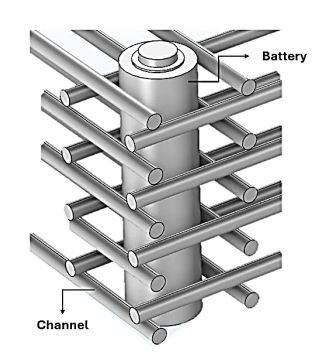
The battery pack consists of an array of batteries, connected each other through an element called busbar. This part links, both in series and parallel, different batteries through the poles. To account for the current inside the material, the following heat generation is added to the energy equation.

$$Q_{irrbb} = \left(\frac{1}{A_{bb}}\right)^2 * \frac{1}{\sigma_{bb}} \tag{5}$$

Where A_{bb} is the cross-section area of the busbar while σ_{bb} is the electric conductivity of the busbar material (copper). Fig. 2 depicts the whole battery pack with all connections. The pack configuration is such that consecutive batteries along the y-direction are oriented in the opposite direction. Thus, busbars in series connect two opposite poles, while those in

parallel connect similar poles. To avoid direct contact between the fluid and the battery, the indirect cooling solution is here presented. Specifically, an array of horizontal tubes is placed around each battery, to create a crossflow configuration, as shown in Fig. 2. The alternate direction of tubes – along the length and depth of the battery – allows the thermal field to be more uniform and it also reduces the peak temperature.





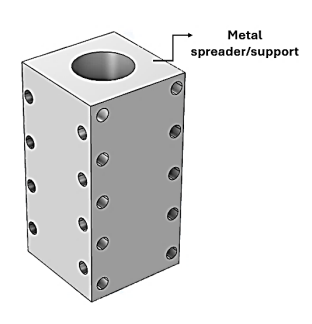


Fig. 2: Top view of Battery pack

In this frame, a relevant assumption is to consider the battery wrapped by a thin layer of electric insulating material, which avoids possible short circuits due a current flow from battery through the metal support without introducing additional thermal resistance. The presented battery pack configuration is more efficient than the alternative ones but demands significantly more energy to drive the water flow. Additionally, the increased material required for the support structure raises the system's cost and makes it considerably heavier. Therefore, the objective is to reduce the weight and cost of the system while maintaining its heat transfer efficiency. To achieve this, topology optimization is applied to strategically allocate material for the support, ensuring it is placed only where required.

3. Topology optimization

This paper applies a density-based topology optimization (TO) approach. The optimization is performed on a portion of the metal support previously shown. Based on thermal and geometry symmetry, the actual design domain is reduced to the one shown in Fig. 3. Starting from the initial support, the actual domain has been computed as 1/8 of the total. The key geometry parameters, *i.e.*, $L'_c = 15$ mm, $L_B = 17$ mm, $H_B = 3.25$ mm and $r_c = 1.0$ mm, are the half the length of the channel, the depth and the height of the support and the channel radius, respectively. Here, q_1 and q_2 are the boundary conditions of heat transfer *i.e.*, the heat flux that simulates the heat source inside the battery and the effect of the presence of water inside the channel. As we perform a steady-state TO, the q_1 value is chosen as the maximum value of heat flux of the unsteady case, while q_2 is the convective heat flux with the heat transfer fluid, computed considering a fluid velocity equal to 0.2 m/s.

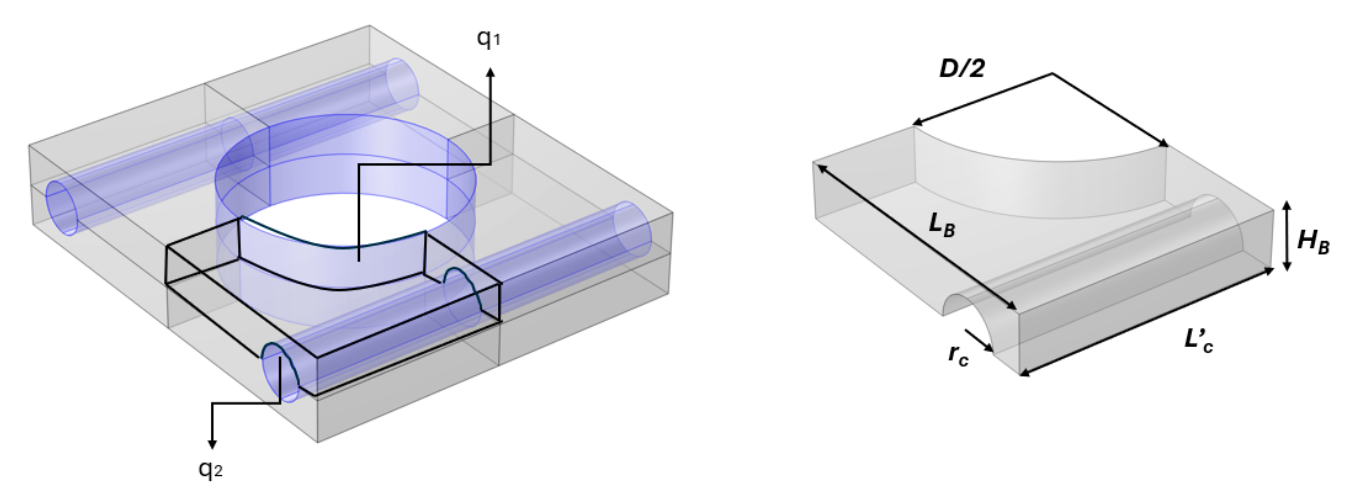


Fig. 3: Initial part of the support and boundary conditions

The governing equation for this case is the heat equation, with

$$\nabla k(\gamma)(\nabla T) = 0 \tag{6}$$

This approach places the material only where it is needed using the design variable (γ). γ can have values between 0 and 1 where: 0 value stands for void, while 1 stands for solid material. The effective thermal conductivity (k) – dependent on γ – is defined as follows, based on the SIMP scheme:

$$k(\gamma) = k_s + (k_f - k_s) \gamma^n \tag{7}$$

Where k_s is the thermal conductivity of solid (aluminium), while k_f is the thermal conductivity of the fluid (water). n is the penalization factor, which varies from 3 to 5. To avoid intermediate values of γ , the Helmholtz filter and hyperbolic tangent projection are applied to the design variable, as follows:

$$-R^2 \nabla^2 \gamma_{fi} + \gamma_{fi} = \gamma_i \tag{8}$$

$$\gamma = \frac{\tanh[\beta(\gamma_{fi} - \gamma_{\beta})] + \tanh(\beta\gamma_{\beta})}{\tanh[\beta(1 - \gamma_{\beta})] + \tanh(\beta\gamma_{\beta})}$$
(9)

where R, γ_{fi} and γ_i represents the filter radius, the filtered design variable and the initial design variable value, respectively. Looking at Eq. (9), γ_{β} is the projection point, set equal to 0.5, while β is the projection slope, which ranges from 8 to 14. All the equations have been computed by method of moving asymptotes (MMA) to update the values of γ and calculate the sensitivity of the objection function. The objective is the average temperature on the cylindrical surface where the battery is placed. The reason for such choice is that the aim is to reduce the surface temperature where the heat flux is set. To achieve this temperature reduction, the TO would place as much solid material as possible. However, to constraint the maximum amount of solid material and thus ensure a lightweight design, a volume fraction (ratio between solid and total volume) of 0.25 is set over the design volume.

4. Results and discussion

This section presents results of baseline and TO cases, providing comparisons in terms of temperature fields inside the metal support and the battery. Fig. 4 shows the temperature distribution for the metal support in both cases and the resulting design of the TO single part. According to this figure, the difference in the maximum temperature reached from both cases is really low, while the significant higher amount of solid material in the baseline case ensures a higher uniformity of the temperature.

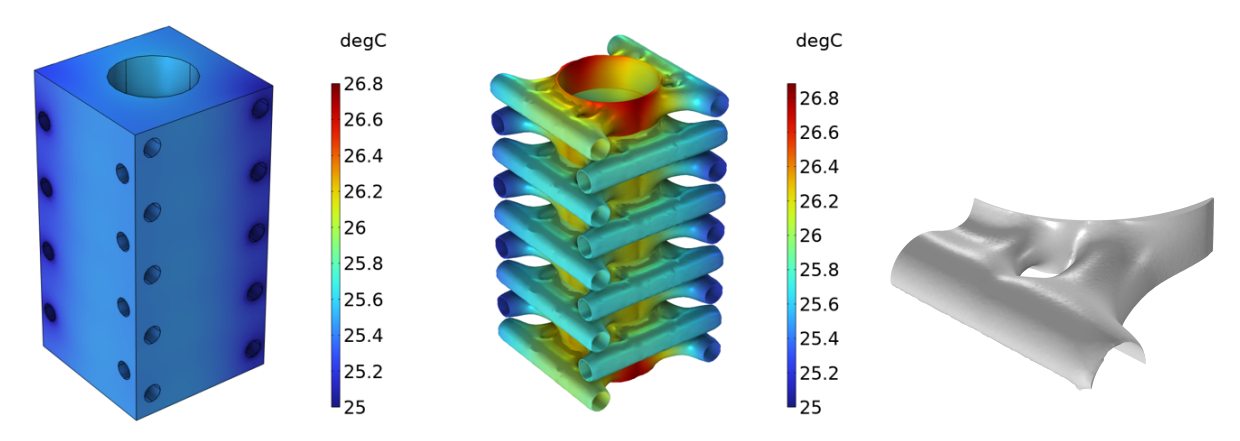


Fig. 4: thermal field of the battery in baseline and TO cases

Fig.5 presents the battery thermal field through a side and bottom view. For the baseline case, those views clearly show that the battery core has an almost one-dimensional temperature distribution, where the temperature decreases from 34 °C to 26 °C. The negative and positive pole are the zones with higher temperature because of the connection with the busbar and the absence of solid material. For the TO case, the maximum temperature reached on the symmetry axis is 38.3 °C.

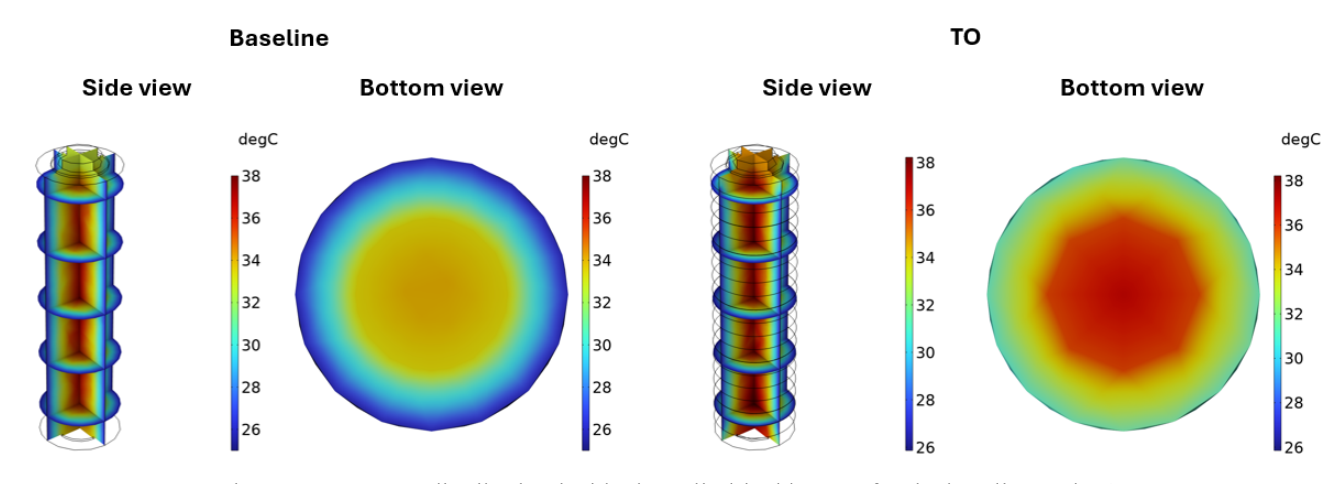


Fig. 5: temperature distribution inside the cylindrical battery for the baseline and TO cases

Finally, Fig. 6 shows the average temperature profiles in time of baseline and TO cases referred to a time period of 1 hour, under a C-rate equal to 10. In particular, these temperatures are computed as average value inside the metal support (left side) and the cylindrical battery (right side).

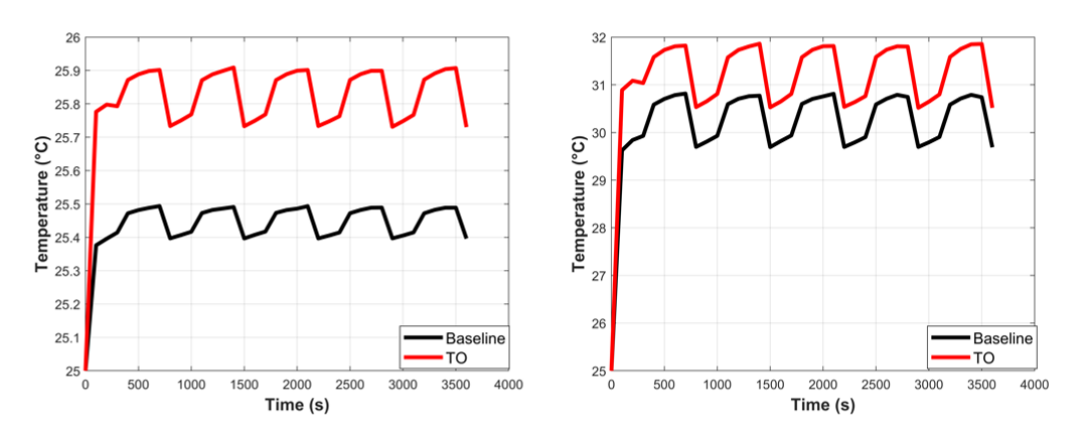


Fig. 6: Average temperatures comparison between baseline case and TO case in support (left) and battery (right)

The average temperature of the battery and the support, as shown in Fig. 8, in the TO case is bigger than Baseline case but increases slightly, in fact the battery temperature is approximately 2 °C higher while the metal support temperature is only 0.5 °C. Table 3 shows the absolute values of different temperature, for baseline and TO, in metal support and battery from which is possible to evaluate the absolute deviation (ε) .

	Metal spreader/support			Battery			
	Baseline	TO	ε	Baseline	TO	ε	
T _{mean} (°C)	25.49	25.90	0.41	30.79	31.85	1.06	
T_{max} (°C)	25.63	26.90	1.27	37.24	38.30	1.06	
Weight (g)	127.0	26.00	101	/	/	/	

Table 3: thermal results of the analyses

The average temperature increases only about 0.4 and 1.0 °C for the metal support and battery, respectively. The increase in the maximum temperature is slightly higher, but always lower than 1.5 °C. The weight reduction is significant, with a decrease of 79.5% compared to the baseline case.

5. Conclusions

This study addresses the thermal challenges encountered during battery operation and proposes a solution through the development of a battery thermal management system (BTMS). A baseline cooling fluid system is initially presented, highlighting its limitations. An innovative design is then introduced – by using topology optimization – aimed at maintaining the battery temperature below the critical threshold, even if slightly higher than that achieved by the baseline. This little drawback is compensated by the notable reduction in the overall weight of the system, without compromising thermal performance. The main conclusions as are follows:

- From baseline case to new solution the temperature of the battery increases but remains below the established limit of 50°C while the thermal field along the battery, not considering the poles, maintain the uniformity but not like the baseline case.
- Thanks to topology optimization, the amount of solid material used for the spreader/support has been reduced by 79.5% with respect to the baseline case, to the detriment of a slight increase of the mean temperature of the battery, *i.e.*, 1 °C.

Future work will involve the exploration of alternative design configurations, which will vary along with the battery height. The influence of different solid material distributions will be investigated by changing the volume fraction constraint. Additionally, simulations will be conducted for various battery pack placements to develop position-specific designs that adapt to changes in the cooling conditions.

Acknowledgment

This work was supported by the Italian Government MUR Grant No. P2022NYPHL – PRIN 2022 PNRR "VISIONS: eVolutIonary deSign of InnOvative heat traNsfer deviceS" – Funded by European Union – Next Generation EU, Mission 4, Component 1, CUP: F53D23009800001

References

- [1] Jie Liu, Saurabh Yadav, Mohammad Salman, Santosh Chavan, Sung Chul Kim. Review of thermal coupled battery models and parameter identification for lithium-ion battery heat generation in EV battery thermal management system.2024
- [2] Shuai Ma, Modi Jiang, Peng Tao, Chengyi Song, Jianbo Wu, Jun Wang, Tao Deng, Wen Shang. Temperature effect and thermal impact in lithium-ion batteries: A review. 2018
- [3] Hrishav Dey, Sukumar Pati, Pitambar R. Randive, László Baranyi. Effect of finned networks in PCM based battery thermal management system for cylindrical Li-ion batteries. 2024
- [4] Peng Qin, Mengran Liao, Wenxi Mei, Jinhua Sun, Qingsong Wang. The experimental and numerical investigation on a hybrid battery thermal management system based on forced-air convection and internal finned structure. 2021
- [5] A novel water-based direct contact cooling system for thermal management of lithium-ion batteries. Tian Zhou, Junhui Wu, Xuan Liu, Xiaolei Jiao, Nianben Zheng, Zhiqiang Sun. 2025
- [6] Mazhar Hussain, Mohd. Kaleem Khan, Il mio amico Manabendra Pathak. Thermal management of high-energy lithium titanate oxide batteries using an effective channeled dielectric fluid immersion cooling system. 2024
- [7] Wenjing Cao, Chunrong Zhao, Yiwei Wang, Ti Dong, Fangming Jiang. Thermal modeling of full-size-scale cylindrical battery pack cooled by channeled liquid flow. 2019
- [8] Peiru Chen a, Liang Gao a, Wei Li b, Jiyun Zhao c, Akhil Garg a,*, Biranchi Panda. A topology optimization-based novel design and comprehensive thermal analysis of a cylindrical battery liquid cooling plate. 2024
- [9] Chun Yang Guo, Mohammed W. Muhieldeen, Kah Hou Teng, Kit Chun Ang, Wei Hong Lim. A novel thermal management system for lithium-ion battery modules combining indirect liquid-cooling with forced air-cooling: Deep learning approach. 2024
- [10] David Martínez-Maradiaga, Alberto Damonte, Alessandro Manzo, Jan H.K. Haertel, Kurt Engelbrecht. Design and testing of topology optimized heat sinks for a tablet. 2019
- [11] Zhenpo Wang, Jun Ma, And Lei Zhang, (Member, IEEE) Finite Element Thermal Model and Simulation for a Cylindrical Li-Ion Battery. 2017